A Facile Method to Fabricate ZnO Hollow Spheres and Their Photocatalytic Property

Ziwei Deng, Min Chen, Guangxin Gu, and Limin Wu*

Department of Materials Science and the Advanced Coatings Research Center of China Educational Ministry, Advanced Materials Laboratory, Fudan University, Shanghai 200433, People's Republic of China

Received: September 24, 2007; In Final Form: October 12, 2007

This paper presents a novel and facile method for the fabrication of ZnO hollow spheres. In this approach, zinc ions were first adsorbed onto the surfaces of sulfonated polystyrene core−shell template spheres, and then reacted with NaOH to form a ZnO crystal nucleus, which was followed by a growth step to form ZnO nanoshells. During the formation of ZnO nanoshells or later on, the template spheres were "dissolved" in the same media to obtain ZnO hollow spheres directly. Neither additional dissolution nor calcination process was needed in this method to remove the templates, and the reaction conditions were very mild: neither high temperature nor long time was needed. Transmission electron microscopy, scanning electron microscopy, X-ray photoelectron spectroscopy, X-ray diffraction, and Brunauer−Emmett−Teller analysis were used to investigate the morphology, surface composition, crystalline structure, specific surface area, and porosity of the ZnO hollow spheres, respectively. UV−visible spectra show that these ZnO hollow spheres had very good photocatalytic activity.

Introduction

Hollow nano- and microspheres with well-defined structures have attracted more and more interest because they have a lot of potential applications in areas such as catalysis, chromatography, protection of biologically active agents, fillers (pigments, coatings), waste removal, and large bimolecular-release systems.[1−7] Since the pioneering works on fabrication of hollow spheres done by Kowalski and colleagues at Rohm and Haas,[8,9] how to fabricate various monodisperse hollow spheres with tailored structural shape and surface properties has remained a great challenge in the area of materials research.

ZnO is a very important wide-band-gap semiconductor with a room-temperature wide band gap of 3.37 eV, which attracts much attention in tailoring its shape and size to optimize the corresponding optical properties. Since ZnO hollow structures can be used in catalysts, delivery vehicles, photomaterials, and chemical and biological sensors, many research efforts have been made to prepare ZnO with hollow structure in recent years.[10−14] For example, Jiang et al.[10] synthesized single-crystalline ZnO polyhedral submicrometer hollow spheres by laser-assisted growth. Mo et al.[15] prepared ZnO nanorod-based hollow microhemisphere assemblies by hydrothermal thermolysis of a zinc ethylenediamine precursor in the presence of the water-soluble long-chain polymer poly(sodium 4-styrenesulfonate) in an aqueous solution, which was sealed and heated at 180 °C for 12 h. Much more research has focused on template technology based on polystyrene (PS),[16,17] carbon spheres,[14] and spherobacteria.[18] In these processes, however, the ZnO nanoshells or ZnO precursors were first deposited onto the surfaces of template spheres to form core−shell composite spheres, then the removal of the template particles by selective dissolution in an appropriate solvent or by calcination at elevated temperature was indispensably carried out to obtain ZnO hollow spheres from the core−shell composite spheres.

* Corresponding author. E-mail: lxw@fudan.ac.cn or lmw@fudan.edu.cn.

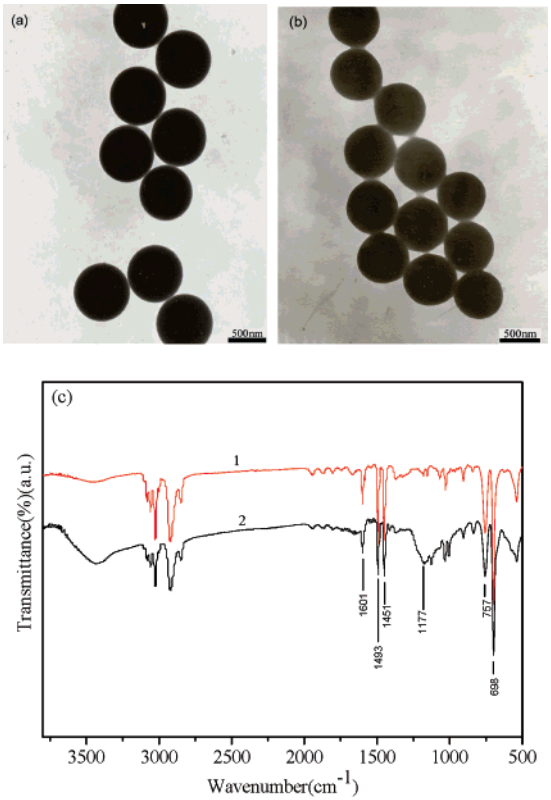

Figure 1. TEM images of the PS spheres (a) and sulfonated PS core−shell gel spheres (b). (c) FTIR spectra of PS spheres (spectrum 1) and sulfonated PS core−shell gel spheres (spectrum 2).

Recently, we reported a facile approach to prepare monodisperse hollow silica or titania spheres via a one-step process.[19−21] In that method, aqueous ammoniacal alcohol was used as the catalyst and medium. Monodisperse positively charged PS particles were prepared by dispersion polymerization using the cationic monomer 2-(methacryloyl)ethyltrimethylammonium chloride as the comonomer, which ensured that the generation

10.1021/jp077662w CCC: $40.75
Published on Web 12/08/2007

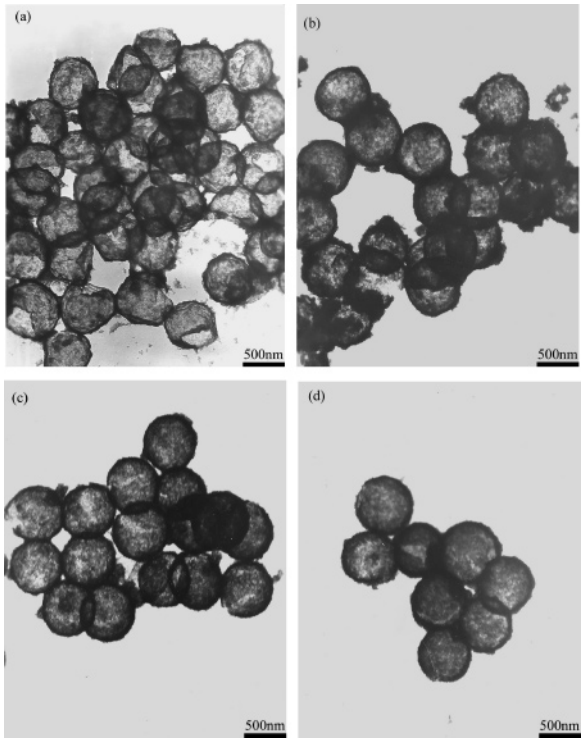

Figure 2. TEM images of ZnO hollow spheres prepared by various NaOH concentrations: (a) 0.025 mol/L; (b) 0.1 mol/L; (c) 0.3 mol/L; (d) 0.4 mol/L. $Zn(Ac)_2 \cdot 2H_2O$: 0.036 mol/L.

of silica or titania sol from the hydrolysis and the condensation of TEOS or tetra-*n*-butyl titanate could be rapidly captured by PS particles via electrostatic interaction in aqueous ammoniacal alcohol medium at 50 °C. Under these conditions, PS particles were "dissolved" subsequently and even synchronously to directly form silica or titania hollow spheres. Namely, the formation of the inorganic shells and the dissolution of core template spheres occurred in the same media; neither additional dissolution nor calcination process was used to remove the PS cores. Ammonia was not only used as the catalyst in the sol−gel reaction of TEOS or tetra-*n*-butyl titanate, but also served as a key parameter to "dissolve" the PS template particles.

In this paper, we further developed a novel and facile method to fabricate ZnO hollow spheres. In this approach, the sulfonated PS core−shell spheres were used as template spheres; when $Zn(Ac)_2 \cdot 2H_2O$ was added into the ethanol dispersion of the template spheres, zinc ions were first adsorbed onto the surfaces of template spheres via electrostatic interaction. As the NaOH solution was added into the mixture and reacted with zinc ions, ZnO nanoshells formed while the sulfonated PS core−shell spheres were "dissolved" in the same media to obtain ZnO hollow spheres directly. Neither additional dissolution nor calcination process was needed to remove the template cores, and the reaction conditions were mild: neither high temperature nor long time was needed. Compared with our previous method,[19−21] this approach has some obvious differences: (i) NaOH served as both a reactant to form ZnO nanoshells as well as an alkali media with ethanol to "dissolve" template spheres, while ammonia in our previous method served as both the catalyst for the hydrolysis and condensation of precursors as well as an alkali media with ethanol to "dissolve" template spheres; (ii) sulfonated PS particles instead of positively charged PS were used as templates; (iii) the formation mechanism of ZnO nanoshells in this approach was also different from that of SiO_2 or TiO_2 nanoshells in our previous method. Transmission electron microscopy (TEM), scanning electron microscopy

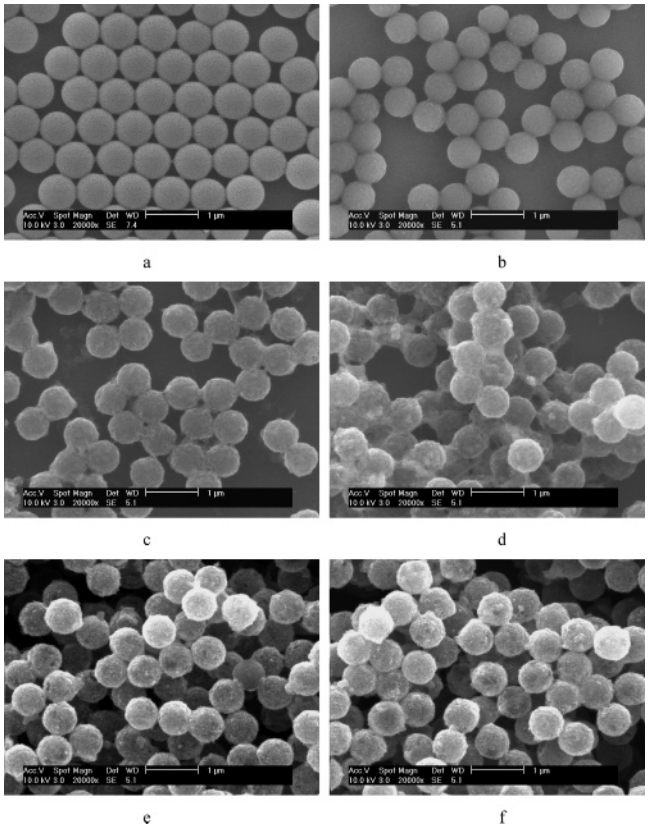

Figure 3. SEM images of PS (a), sulfonated PS core−shell gel spheres (b), and ZnO hollow spheres prepared by various concentrations of NaOH: (c) 0.025 mol/L, (d) 0.1 mol/L, (e) 0.3 mol/L, and (f) 0.4 mol/L. $Zn(Ac)_2 \cdot 2H_2O$: 0.036 mol/L.

(SEM), X-ray photoelectron spectroscopy (XPS), X-ray diffraction (XRD), and Brunauer−Emmett−Teller (BET) analysis were used to investigate the morphology, surface composition, crystalline structure, specific surface area, and porosity of the ZnO hollow spheres, respectively. UV−visible spectrometer analyses showed that the ZnO hollow spheres had very good photocatalytic activity.

Experimental Section

Materials. Poly(vinylpyrrolidone) (PVP, MW = 40 000) was purchased from Fluka (U.S.A.) and used as received. Styrene was purchased from Shanghai Chemical Reagent Co. (China) and distilled to remove the inhibitor in a vacuum and stored at 4 °C until use. 2,2′-Azobisisobutyronitrile (AIBN) was purified by recrystallization in ethanol. Sulfuric acid (H_2SO_4,98%), sodium hydroxide (NaOH), zinc acetate dihydrate ($Zn(Ac)_2 \cdot 2H_2O$), rhodamine B(RB), reactive brilliant red K-2BP(BR K-2BP), absolute ethanol, and commercial ZnO powders were purchased from Shanghai Chemical Reagent Co. (China) and used as received. Ultrapure water (>17 MΩ cm^{-1}) from a Milli-Q water system was used throughout the experiment.

Preparation of Monodisperse PS Spheres. Monodisperse PS spheres were prepared by dispersion polymerization described as follows: Styrene (10.0 g), PVP (3.0 g), AIBN (0.2 g), ethanol (75.0 g), and water (25.0 g) were added into a 250 mL four-neck round-bottomed flask equipped with a mechanical stirrer, a thermometer with a temperature controller, a N_2 inlet, a Graham condenser and a heating mantle. The reaction solution was deoxygenated by bubbling nitrogen gas at room temperature for ca. 60 min and then reacted at 70 °C for 24 h under a stirring

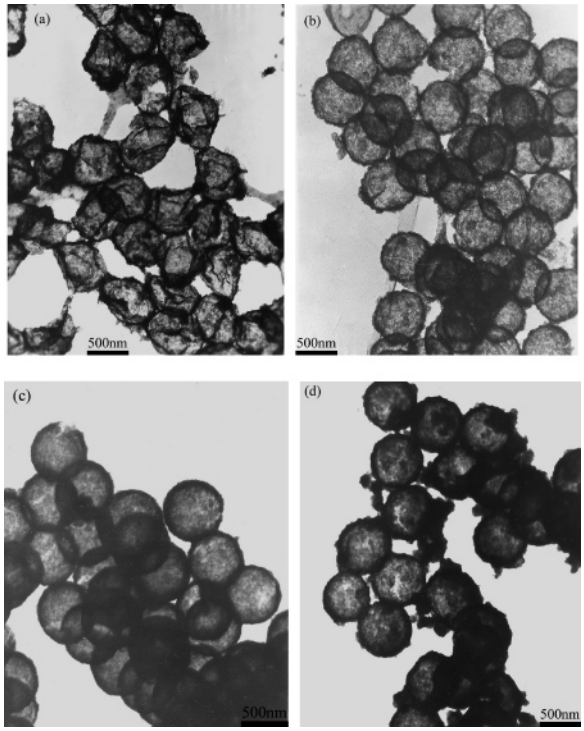

Figure 4. TEM images of ZnO hollow spheres prepared by various concentrations of $Zn(Ac)_2 \cdot 2H_2O$: (a) 0.009 mol/L, (b) 0.018 mol/L, (c) 0.036 mol/L, and (d) 0.055 mol/L. NaOH: 0.2 mol/L.

rate of 100 rpm. The dispersion was centrifuged and dried in a vacuum oven at room temperature for 24 h to obtain the PS powders.

Preparation of Sulfonated PS Core−Shell Spheres. The dried PS powder (3.0 g) was immersed in concentrated sulfuric acid (98%, 30 mL) and stirred at 40 °C for 4 h to form sulfonated PS core−shell gel spheres, which were separated by centrifugation (10 000 rpm) from the system, washed with a large excess of ethanol, and then redispersed in ethanol for subsequent use.

Preparation of ZnO Hollow Spheres. A 10.0 g portion of the sulfonated PS core−shell gel sphere dispersion (with 1% solid content) was added into 25 mL of the $Zn(Ac)_2 \cdot 2H_2O$ ethanol solution and stirred at 60 °C for 1 h, then 25 mL of a NaOH ethanol solution was dropped into the mixture and stirred at 60 °C for another 2 h to obtain ZnO hollow spheres directly. The concentrations of both the $Zn(Ac)_2 \cdot 2H_2O$ and NaOH ethanol solutions varied.

Photocatalytic Property. The obtained ZnO hollow spheres were separated from the reaction mixture by centrifugation, washed several times with ethanol and ultrapure water to remove impurities, dried in a vacuum oven for 12 h, and used as photocatalysts for the degradation of different dyes. In the photocatalytic activity experiments, a cylindrical pyrex flask was used as the photoreactor vessel, 30 mg of ZnO hollow sphere powder was added into 30 mL of the dye solution (5×10^{-5} mol/L), and the mixture was magnetically stirred in the dark for 30 min to ensure the adsorption/desorption equilibrium of dyes with the ZnO hollow spheres, followed by exposure to a 40 W mercury lamp (SPETROLINKER XLE-1000A UV-lamps, $\lambda = 365$ nm, illumination power = 2500−3100 $\mu W/cm^2$). The analytic samples exposed for different times were taken out from the reaction suspension and centrifuged at 15 000 rpm for 15 min to remove the ZnO particles, then were monitored by a UV−visible spectrophotometer. The photocatalytic property of commercial ZnO powders was also monitored for the sake of comparison.

Characterization. *TEM Observation.* TEM (Hitachi H-800, Hitachi Corp.) was used to observe the morphologies of the obtained spheres. The dispersions were diluted with ethanol and ultrasonicated at 25 °C for 10 min and then dried onto carbon-coated copper grids before examination.

Fourier Transform Infrared (FTIR) Measurement. FTIR spectra were taken on a Nexus 470 FTIR spectrometer (Nicolet Instruments, Madison, WI). The sphere dispersions were centrifuged and washed by absolute ethanol, then dried in a vacuum oven and pressed into KBr pellets for FTIR measurement.

SEM Observation. (1) The morphologies of the ZnO hollow spheres were further characterized by SEM (Philips XL30 apparatus). The dispersions of the ZnO hollow spheres were diluted with absolute ethanol and dried on a cover glass for examination. (2) The typical ZnO hollow spheres were dehydrated and subsequently embedded in epoxy for microtoming, the obtained ultrathin sections were sputter-coated with gold, and then the morphologies of the broken ZnO hollow spheres were observed by SEM.

XPS. XPS measurement was carried out on a PHI-5000C ESCA system with Mg Kα radiation ($h\nu = 1253.6$ eV); the X-ray anode was run at 250 W, and the high voltage was kept at 14.0 kV with a detection angle of 54°. All the binding energies were calibrated by using the containment carbon (C1s = 284.6 eV).

XRD. Crystal structure identification was carried out using a Rigaku D/max-rB X-ray diffractometer with Cu Kα irradiation ($\lambda = 1.54056$ Å) at a scanning rate of 0.02 deg/s in 2θ ranging from 20° to 80°. The samples for XRD were supported on a glass substrate.

BET Analysis. Nitrogen adsorption−desorption measurements were performed at 77 K using an ASAP 2010 analyzer utilizing the BET model for the calculation of surface areas. The pore size distribution was calculated from the adsorption isotherm curves using the Barrett−Joyner−Halenda (BJH) method.

UV−Visible Spectrum. UV−visible absorption spectra were recorded using a UV−visible spectrophotometer (Hitachi UV-3000, Japan). The samples were placed in a 1 cm × 1 cm × 3 cm quartz cuvette, and spectra were recorded at room temperature.

Results and Discussion

Sulfonated PS Core−Shell Gel Template Spheres. The TEM image of the original PS spheres prepared via dispersion polymerization indicates that all these PS spheres were monodisperse and had smooth surfaces, as shown in Figure 1a. Figure 1b displays that sulfonation obviously did not change the average particle size of PS spheres since the sulfonation reaction occurred inwardly from the surfaces of the PS spheres.[22,23] A new absorbance band at 1177 cm^{-1} attributed to the absorption vibration of the $-SO_3H$ groups was observed on the FTIR spectrum of sulfonated PS core−shell gel spheres compared with the FTIR spectrum of original PS spheres (the peaks at 698, 757, 1451, 1493, and 1601 cm^{-1} for PS), as demonstrated in Figure 1c, confirming that the sulfonated PS spheres indeed had $-SO_3H$ groups.

Effect of the NaOH Concentrations. After the sulfonated PS core−shell gel spheres were used as templates and adsorbed by zinc ions from $Zn(Ac)_2 \cdot 2H_2O$ ethanol solution via electrostatic interaction between $-SO_3H$ groups and zinc ions, various

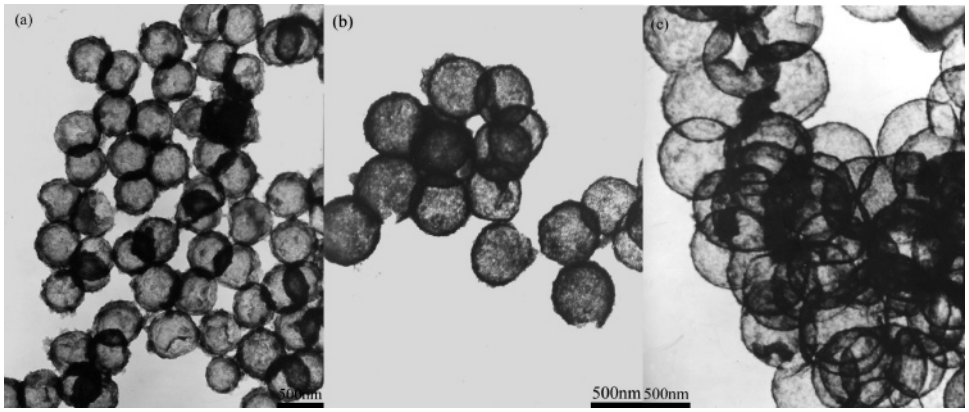

Figure 5. TEM images of ZnO hollow spheres prepared by different sizes of templates: (a) 450 nm, (b) 700 nm, and (c) 1100 nm.

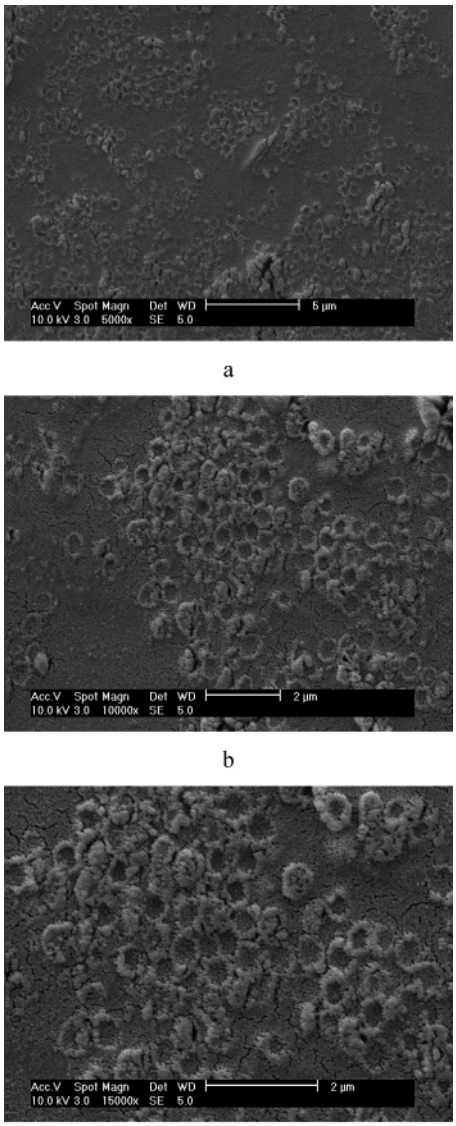

Figure 6. SEM images of the broken ZnO hollow spheres observed at different magnifications: (a) ×5000, (b) ×10000, and (c) ×15000.

concentrations of NaOH ethanol solution were added into the dispersion and reacted at 60 °C for 2 h, forming ZnO nanoshells on the surfaces of the templates since zinc ions could react with NaOH, causing the formation of ZnO nanoparticles.[24,25] Very interestingly, the sulfonated PS core−shell gel spheres were "dissolved" in the alkaline ethanol media at 60 °C subsequently

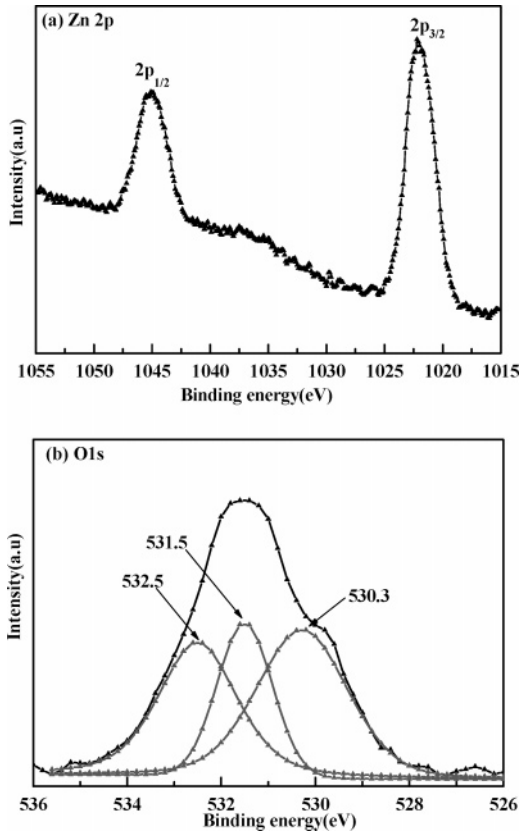

Figure 7. XPS spectra of typical ZnO hollow spheres: (a) Zn 2p spectrum; (b) O 1s spectrum.

and even synchronously to form ZnO hollow spheres directly, as indicated in Figure 2, which was very similar to our previous works on the fabrication of SiO_2 and TiO_2 hollow spheres using positively charged PS as templates and aqueous ammoniacal alcohol as the medium.[19−21] The big differences between this approach and our previous method are: (i) NaOH served as both a reactant to form ZnO nanoshells as well as an alkali media with ethanol to "dissolve" template spheres, while ammonia in our previous method served both as the catalyst for the hydrolysis and condensation of TEOS or tetra-*n*-butyl titanate and as an alkali medium with ethanol to "dissolve" template spheres; (ii) the formation mechanism of ZnO nanoshells in this approach was quite different from that of SiO_2 or TiO_2 nanoshells in our previous method. Figure 2 also displays some broken or deformed ZnO hollow spheres prepared at lower NaOH concentrations, probably because the relatively thinner ZnO shells could not endure the strike from the electron beam with the high voltage of TEM.

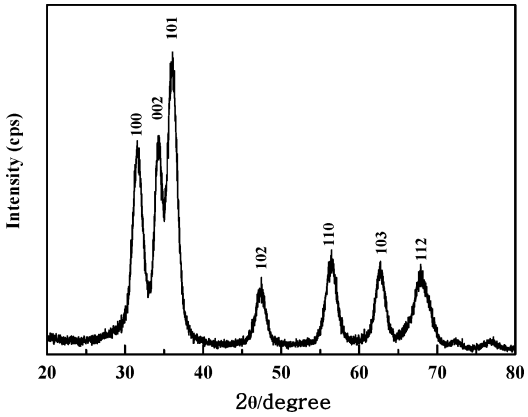

Figure 8. XRD patterns of typical ZnO hollow spheres.

Figure 3 illustrates the SEM images of the original PS, sulfonated PS core−shell gel spheres, and ZnO hollow spheres prepared at various NaOH concentrations. Compared with the original PS spheres and sulfonated PS core−shell gel spheres, relatively rougher surfaces were observed for all ZnO hollow spheres.

Effect of the $Zn(Ac)_2{\cdot}2H_2O$ Concentrations. Figure 4 further demonstrates the TEM images of ZnO hollow spheres prepared from different concentrations of $Zn(Ac)_2{\cdot}2H_2O$ ethanol solution. When the concentration of $Zn(Ac)_2{\cdot}2H_2O$ was 0.009 mol/L, the ZnO nanoshells were very thin, resulting in many deformed or broken ZnO hollow spheres (see Figure 4a). When the concentration of $Zn(Ac)_2{\cdot}2H_2O$ was increased to 0.018 and 0.036 mol/L, ZnO hollow spheres with wall thicknesses of ∼20 and ∼50 nm (measured from the cross-section SEM images of ZnO hollow spheres[19]) were obtained (see Figure 4b,c), respectively. As the concentration of $Zn(Ac)_2{\cdot}2H_2O$ was further increased to 0.055 mol/L, the wall thickness of the ZnO hollow spheres was increased to ∼65 nm, but some agglomerates of ZnO nanoparticles were also observed in addition to hollow spheres (see Figure 4d), suggesting that the sulfonated PS core−shell gel spheres were unable to adsorb all the zinc ions absolutely and equably at higher $Zn(Ac)_2{\cdot}2H_2O$ concentrations; some free zinc ions reacted with NaOH, causing agglomerates of ZnO nanoparticles. Thus, the wall thickness of the ZnO hollow spheres could be easily tailored by simply altering the concentration of $Zn(Ac)_2{\cdot}2H_2O$.

Effect of the Size of Template Spheres. ZnO hollow spheres with different sizes could be prepared using various sizes of sulfonated PS core−shell gel spheres as templates, as shown in Figure 5.

In order to further confirm the hollow structures of the ZnO spheres, the typical ZnO hollow spheres were dehydrated and embedded in epoxy for microtoming, the obtained ultrathin sections were observed by SEM, and the hollow structure could be seen clearly, as shown in Figure 6.

XPS Measurements. The typical hollow spheres were scanned by XPS, and their survey curves are illustrated in Figure 7. The binding energies of both Zn $2p_{1/2}$(1045.1 eV) and Zn $2p_{3/2}$ (1022.2 eV), as indicated in Figure 7a, were slightly larger than the values of Zn in the bulk ZnO, indicating that Zn was in the formal Zn^{2+} valence state within an oxygen-deficient environment.[26,27]

The deconvolution of the XPS spectrum of the O1s core level line showed three different peaks, as demonstrated in Figure 7b. The peak centered at 530.3 eV was associated with the O^{2-} ions in the wurtzite structure surrounded by the Zn atoms with their full complement of nearest-neighbor O^{2-} ions,[28,29] the peak

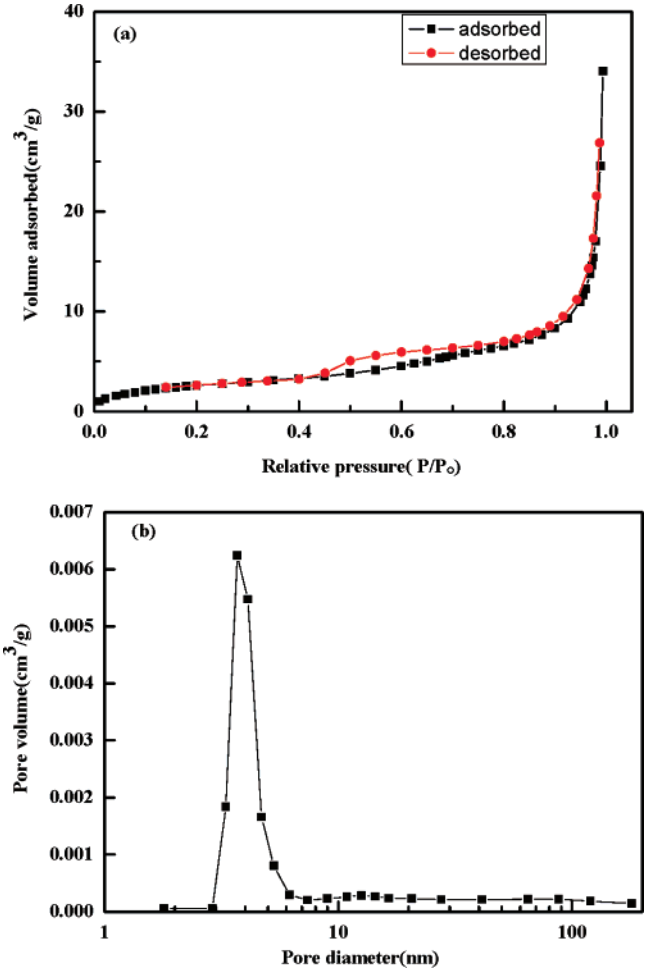

Figure 9. (a) Nitrogen adsorption/desorption isotherm and (b) BJH pore size distribution of ZnO hollow spheres.

Figure 10. Diagram of the formation mechanism of the ZnO hollow spheres.

at 531.5 eV was associated with the O^{2-} ions in the oxygen-deficient regions within the matrix of ZnO,[27,28] and the binding energy peak at 532.5 eV was attributed to the loosely bound oxygen, such as adsorbed O_2 or adsorbed H_2O, on the ZnO surface.[30,31]

XRD Patterns. Figure 8 further presents the XRD patterns of the typical ZnO hollow spheres. The diffraction peaks were quite similar to those of bulk ZnO, which could be indexed as the hexagonal wurtzite structure of ZnO. The calculated lattice constants were $a = 3.25$ Å and $c = 5.21$ Å, which were in good agreement with the JCPDS file of ZnO (JCPDS No. 36-1451). The average crystallite size was around 6.1 nm according to the Scherrer−Warren formula, indicating that ZnO hollow spheres were made of those ZnO nanocrystals.

Surface Areas and Porosity. The N_2 adsorption−desorption isotherm and the pore-size distribution of ZnO hollow spheres are shown in Figure 9, which confirms the presence of porous structures of prepared ZnO hollow spheres. The BET specific surface area and the average pore size of the ZnO hollow spheres were around 9.77 m^2/g and 18.3 nm, respectively, while those of the commercial ZnO powders were 3.64 m^2/g and 28.9 nm (see Supporting Information, S1), respectively. Obviously, the

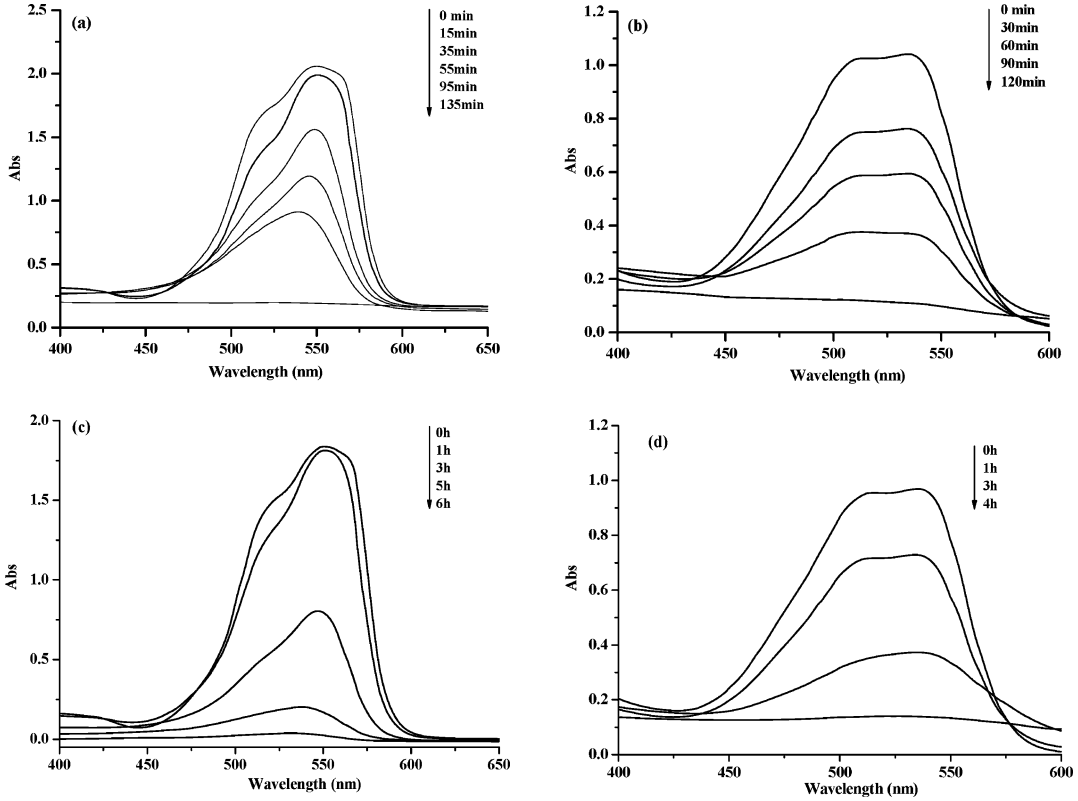

Figure 11. UV−visible spectra of the solutions at 5×10^{-5} mol/L of RB (a,c) and BR K-2BP (b,d) in the presence of (a,b) ZnO hollow spheres (30 mg) and (c,d) commercial ZnO powders (30 mg).

ZnO hollow spheres had bigger specific surface areas and smaller average pore sizes than the commercial ZnO powders.

Formation Mechanism. To further understand the formation mechanism of ZnO hollow spheres in this study, a control experiment with all the ingredients kept the same but without $Zn(Ac)_2 \cdot 2H_2O$ was carried out. When the sulfonated PS core−shell gel spheres were stirred in NaOH ethanol medium at 60 °C for 2 h, no sulfonated PS core−shell gel spheres were observed by TEM, confirming that the template spheres could indeed be "dissolved" in NaOH/ethanol media at 60 °C.

On the basis of the above research and the control experiment, a possible formation mechanism of ZnO hollow spheres could be described in Figure 10. When $Zn(Ac)_2 \cdot 2H_2O$ solution was added into the dispersion of sulfonated PS core−shell gel spheres, the zinc ions were adsorbed onto the surfaces of sulfonated PS core−shell gel spheres through electrostatic attraction. With the addition of NaOH solution, the adsorbed zinc ions first reacted with NaOH to form a ZnO crystal nucleus on the sulfonated PS core−shell gel spheres during this nucleation step. Then the ZnO crystal nucleus grew by the growth step to form the ZnO nanoshells on the template spheres. During this process or later on, the template spheres were "dissolved" in alkaline ethanol medium. These "dissolved" PS macromolecule chains and/or their aggregates diffused out through the porous ZnO nanoshells, forming ZnO hollow spheres.

Photocatalytic Property of ZnO Hollow Spheres. Dyes are an abundant class of synthetic, colored compounds that present a danger to the environment because they are toxic and very stable (and thus resistant to aerobic degradation).[32,33] Considering these environmental problems, oxide semiconductors, such as TiO_2[34−36] and ZnO,[36−39] are used as promising photocatalysts for the mineralization of these organic pollutants. Although they both exhibit high photocatalytic activities, ZnO has been shown to be more efficient in the photodegradation of dyes under UV-light illumination.[34,35] For instance, Lizama et al.[34] optimized the photodegradation of reactive blue 19 on ZnO and TiO_2 commercial powders by using the factorial design method and showed that ZnO was a more efficient catalyst than TiO_2. Sakthivel et al.[35] also compared the efficiency of different semiconductor photocatalysts (TiO_2, ZnO, SnO_2, ZrO_2, α-Fe_2O_3, WO_3, and CdS) in the photodegradation of acid brown 14 in an aqueous solution using sunlight as the energy source. From this comparative study, ZnO emerged as the most active photocatalyst.

Here we preliminarily investigated the photocatalytic activities of the dyes degraded by prepared ZnO hollow spheres compared with the commercial ZnO powders. Two different kinds of dyes—RB (basic dye) and BR K-2BP (reactive dye)—were selected, and their evolutions of the UV−visible spectra at the wavelength of the absorbance maximum (λ_{max}) during the degradation are illustrated in Figure 11. Under UV-light irradiation, the absorption peaks of both RB and BR K-2BP aqueous solutions in the presence of ZnO hollow spheres diminished gradually as the exposure time increased. After exposure for 135 min and 120 min for RB and BR K-2BP, respectively, the absorption peaks disappeared completely, indicating the complete photocatalytic degradation of the dyes (see Figure 11a,b). Compared with the UV−visible spectra of the photocatalytic degradation of RB and BR K-2BP by commercial ZnO powders (see Figure 11c,d), the prepared ZnO hollow spheres had considerably higher photocatalytic activity for the degradation of dyes than the commercial ZnO powders. This should be attributed to the larger specific surface area of ZnO hollow spheres.

The photocatalytic activity of ZnO hollow spheres could be further confirmed by two control experiments, which are presented in the Supporting Information. One was carried out

in the absence of the ZnO hollow spheres; the color of the dyes remained unchanged, even after UV irradiation for 24 h (see Supporting Information, Figures S3a and S4a). Another was done in the dark in the presence of the ZnO hollow spheres; the absorbance at λ_{max} of the dyes decreased very slightly (see Supporting Information, Figures S3b and S4b). This evidence confirmed that the ZnO hollow spheres had very good photocatalytic activity.

The photocatalytic mechanism could be explained as follows: The conduction-band electrons (e_{cb}^-) and valence-band holes (h_{vb}^+) are generated on the surfaces of ZnO nanoparticles when an aqueous suspension of ZnO hollow spheres is illuminated by UV light with energy greater than the band gap energy. Holes can react with water adhering to the surfaces of ZnO nanoparticles to form highly reactive hydroxyl radicals ($OH^•$), while oxygen acts as an electron acceptor by forming a super-oxide radical anion ($O_2^•$). These super-oxide radical anions further form hydroxyl radicals, whose powerful oxidation ability can degrade organic dye.[40]

Conclusion

On the basis of this study, the ZnO hollow spheres could be prepared using a very simple process. In this method, sulfonated PS core−shell gel spheres were used as templates, and the zinc ions were first adsorbed onto the surfaces of template spheres via electrostatic interaction and then reacted with NaOH to form a ZnO crystal nucleus, which was followed by the growth step to form ZnO nanoshells. The sulfonated PS core−shell gel spheres were "dissolved" in the same media during the coating process or later on to form ZnO hollow spheres directly. The wall thickness and the size of the ZnO hollow spheres could be easily tailored by altering the concentration of $Zn(Ac)_2 \cdot 2H_2O$ and the size of the template spheres, respectively. Preliminary studies showed that these ZnO hollow spheres had very good photocatalytic activity.

This method could be further used to prepare other inorganic hollow spheres, especially metal oxides or metal sulfides (e.g., TiO_2, ZnS, SnO_2, etc.) for different potential applications.

Acknowledgment. The financial support from the Foundation of Science and Technology of Shanghai (07DJ14004), the Shanghai Leading Academic Discipline Project (B113), and the Shuguang Scholar-Tracking Foundation of Shanghai for this research is appreciated.

Supporting Information Available: Nitrogen adsorption/desorption isotherm, pore size distribution, and TEM image of commercial ZnO powders. UV−visible spectra of RB and BR K-2BP solutions exposed to UV light in the absence of ZnO hollow spheres and stirred in the dark in the presence of ZnO hollow spheres. This information is available free of charge via the Internet at http://pubs.acs.org.

References and Notes

(1) Caruso, F.; Caruso, R. A.; Mohwald, H. *Science* **1998**, *282*, 1111.
(2) Jiang, P.; Bertone, J. F.; Colvin, V. L. *Science* **2001**, *291*, 453.
(3) Kim, S. W.; Kim, M.; Lee, W. Y.; Hyeon, T. *J. Am. Chem. Soc.* **2002**, *124*, 7642.
(4) Xu, X.; Asher, S. A. *J. Am. Chem. Soc.* **2004**, *126*, 7940.
(5) Wang, Y.; Cai, L.; Xia, Y. *Adv. Mater.* **2005**, *17*, 473.
(6) Zhu, Y. F.; Shi, J. L.; Shen, W. H.; Dong, X. P.; Feng, J. W.; Ruan, M. L.; Li, Y. S. *Angew. Chem., Int. Ed.* **2005**, *44*, 5083.
(7) Li, Y. S.; Shi, J. L.; Hua, Z. L.; Chen, H. R.; Ruan, M. L.; Yan, D. S. *Nano Lett.* **2003**, *3*, 609.
(8) Kowalski, A.; Vogel, M.; Blankenship, R. M. U.S. Patent 4427836, 1984.
(9) Blankenship, R. M. U.S. Patent 5494971, 1996.
(10) Jiang, Z. Y.; Xie, Z. X.; Zhang, X. H.; Lin, S. C.; Xu, T.; Xie, S. Y.; Huang, R. B.; Zheng, L. S. *Adv. Mater.* **2004**, *16*, 904.
(11) Gao, P. X.; Wang, Z. L. *J. Am. Chem. Soc.* **2003**, *125*, 11299.
(12) Yan, C. L.; Xue, D. F. *J. Phys. Chem. B* **2006**, *110*, 7102.
(13) Yan, L.; C.; Xue, D. F. *J. Phys. Chem. B* **2006**, *110*, 11076.
(14) Wang, X.; Hu, P.; Fangli, Y.; Yu, L. *J. Phys. Chem. C* **2007**, *111*, 6706.
(15) Mo, M. S.; Yu, J. C.; Zhang, L. Z.; Li, S. K. A. *Adv. Mater.* **2005**, *17*, 756.
(16) Agrawal, M.; Pich, A.; Zafeiropoulos, N. E.; Gupta, S.; Pionteck, J.; Simon, F.; Stamm, M. *Chem. Mater.* **2007**, *19*, 1845.
(17) Neves, M. C.; Trindade, T.; Timmons, A. M. B.; Pedrosa de Jesus, J. D. *Mater. Res. Bull.* **2001**, *36*, 1099.
(18) Zhou, H.; Fan, T. X.; Zhang, D. *Microporous Mesoporous Mater.* **2007**, 100, 322.
(19) Chen, M.; Wu, L. M.; Zhou, S. X.; You, B. *Adv. Mater.* **2006**, *18*, 801.
(20) Deng, Z. W.; Chen, M.; Zhou, S. X.; You, B.; Wu, L. M. *Langmuir* **2006**, *22*, 6403.
(21) Cheng, X. J.; Chen, M.; Wu, L. M.; Gu, G. X. *Langmuir* **2006**, *22*, 3858.
(22) Yang, Z. Z.; Li, D.; Rong, J. H.; Yan, W. D.; Niu, Z. W. *Macromol. Mater. Eng.* **2002**, *287*, 627.
(23) Yang, Z. Z.; Niu, Z. W.; Lu, Y. F.; Hu, Z. B.; Han, C. C. *Angew. Chem., Int. Ed.* **2003**, *42*, 1943.
(24) Spanhel.L.; Anderson, M. A. *J. Am. Chem. Soc.* **1991**, *113*, 2826.
(25) Hu, Z. S.; Oskam, G.; Penn, R. L.; Pesika, N.; Searson, P. C. *J. Phys. Chem. B* **2003**, *107*, 3124.
(26) Major, S.; Kumar, S.; Bhatnagar, M.; Chopra, K. L. *Appl. Phys. Lett.* **1986**, *49*, 394.
(27) Peng, Y. Y.; Hsieh, T. E.; Hsu, C. H. *Nanotechnology* **2006**, *17*, 174.
(28) Ramgir, N. S.; Late, D. J.; Bhise, A. B.; More, M. A.; Mulla, I. S.; Joag, D. S.; Vijayamohanan, K. *J. Phys. Chem. B* **2006**, *110*, 18236.
(29) Ye, J. D.; Gu, S. L.; Qin, F.; Zhu, S. M.; Liu, S. M.; Zhou, X.; Liu, W.; Hu, L. Q.; Zhang, R.; Shi, Y.; Zheng, Y. D.; Ye, Y. D. *Appl. Phys. A* **2005**, *81*, 809.
(30) Chen, M.; Wang, X.; Yu, Y. H.; Pei, Z. L.; Bai, X. D.; Sun, C.; Huang, R. F.; Wen, L. S. *Appl. Surf. Sci.* **2000**, *158*, 134.
(31) Coppa, B. J.; Davis, R. F.; Nemanich, R. J. *Appl. Phys. Lett.* **2003**, *82*, 400.
(32) Stylidi, M.; Kondarides, D. I.; Verykios, X. E. *Appl. Catal. B: Environ.* **2003**, *40*, 271.
(33) Bonancêa, C. E.; do Nascimento, G. M.; de Souza, M. L.; Temperini, M. L. A.; Corio, P. *Appl. Catal. B: Environ.* **2006**, *69*, 34.
(34) Lizama, C.; Freer, J.; Baeza, J.; Mansilla, H. D. *Catal. Today* **2002**, *76*, 235.
(35) Sakthivel, S.; Neppolian, B.; Shankar, M. V.; Arabindoo, B.; Palanichamy, M.; Murugesan, V. *Sol. Energy Mater. Sol. Cells* **2003**, *77*, 65.
(36) Vincente, J. P.; Gacoin, T.; Barboux, P.; Boilot, J. P.; Rondet, M.; Guéneau, L. *Int. J. Photoenergy* **2003**, *5*, 95.
(37) Pal, B.; Sharon, M. *Mater. Chem. Phys.* **2002**, *76*, 82.
(38) Wang, H. H.; Xie, C. S.; Zhang, W.; Cai, S. Z.; Yang, Z. H.; Gui, Y. H. *J. Hazard. Mater.* **2006**, *141*, 645.
(39) Pauporte, T.; Rathousky, J. *J. Phys. Chem. C* **2007**, *111*, 7639.
(40) Hoffmann, M. R.; Martin, S. T.; Choi, W.; Bahnemann, D. W. *Chem. Rev.* **1995**, *95*, 69.